

# Two-photon Exchange Corrections to Single Spin Asymmetry of Neutron and $^3\text{He}$

Dian-Yong Chen<sup>1,2\*</sup>, Yu-Bing Dong<sup>3,4</sup>

<sup>1</sup>Research Center for Hadron and CSR Physics, Lanzhou University  
& Institute of Modern Physics of CAS, Lanzhou 73000, China

<sup>2</sup>Institute of Modern Physics,  
Chinese Academy of Science, Lanzhou, 730000, China

<sup>3</sup>Institute of High Energy Physics,  
Chinese Academy of Science, Beijing, 100049, China

<sup>4</sup>Theoretical Physics Center for Science Facilities, CAS, Beijing 100049, China

## Abstract

In a simple hadronic model, the two-photon exchange contributions to the single spin asymmetries for the nucleon and the  $^3\text{He}$  are estimated. The results show that the elastic contributions of two-photon exchange to the single spin asymmetries for the nucleon are rather small while those for the  $^3\text{He}$  are relatively large. Besides the strong angular dependence, the two-photon contributions to the single spin asymmetry for the  $^3\text{He}$  are very sensitive to the momentum transfer.

**PACS numbers:** 13.40.Gp, 13.60.-r, 25.30.-c.

**Key words:** Simple Hadronic Model, Two-Photon Exchange, Single Spin Asymmetry.

## 1 Introduction

In recent years, the two-photon exchange (TPE) effect on the electron-nucleon scattering process attracts many interests again after its success in recoiling the discrepancy of the form factor ratio caused by different experimental extraction techniques [1–6]. The newly estimate results showed that the TPE correction is rather important in extracting the proton's form factors from Rosenbluth separation because of its explicit angle dependence. In addition to explaining the form factor ratio discrepancy, further calculations have emphasized the direct connection between the TPE process and the single spin asymmetry (SSA),  $A_y$ . For the elastic scattering process, this asymmetry is expected to be vanishing in the one photon exchange approximation due to time-reversal invariance. However, it can receive non-zero contributions from the interference between the one-photon exchange amplitude and the imaginary part of the TPE amplitude. That means a nonzero  $A_y$  should be a strong evidence for the exist of the TPE contributions. Since the Born contribution is not present, the measurements of  $A_y$  would provide a unique opportunity to access the information on nucleon structure through the dynamics of the TPE. Recently, in the Jefferson Lab, an experiment was designed to measure the single spin asymmetry of neutron using a vertically polarized  $^3\text{He}$  target [7]. Since free neutron targets do not exist in nature, one has to consider nucleon bound systems, such as deuteron [8] or  $^3\text{He}$  [9]. For the latter case, within a naive model and with only a symmetric S-wave component in the bound state, the two protons have opposite spins and therefore one should expect that the electromagnetic polarized response of the  $^3\text{He}$  essentially is the neutron one.

Theoretically, some calculations about the TPE corrections to the SSAs for nucleon target have been performed in both the simple hadronic model [10] and the parton model [6]. In the latter approach, the

---

\*E-mail: chendy@impcas.ac.cn

results showed that at  $Q^2 = 6 \text{ GeV}^2$  the TPE contributions to the SSA for the proton is of order 1%, and for the neutron, at  $Q^2 = 4.3 \text{ GeV}^2$ , the SSA is somewhat larger than those for the proton [6]. In large momentum transfer region, the electron-nucleon scattering can be considered through the scattering off partons in the nucleon, and well described by the generalized parton distribution functions. However, the experiment designed in the Jefferson Lab was concerned to the single spin asymmetry for the neutron under  $1 \text{ GeV}^2$ . In such low  $Q^2$  range, we believe the simple hadronic model should be more efficient to consider the TPE contributions. In this model, the SSA for the proton target has been evaluated [10] and in present work we further estimate the TPE corrections to the SSAs for the neutron and the  $^3\text{He}$  targets.

This paper is organized as follows. We present some analytical representations of the TPE contributions to the SSAs for the nucleon and the  $^3\text{He}$  within the simple hadronic model in the following section. In section 3, some numerical results and discussions about the TPE contributions to the SSAs for the nucleon and the  $^3\text{He}$  targets are presented.

## 2 TPE Contributions to the SSAs for Neutron and $^3\text{He}$

The  $^3\text{He}$  is also spin-1/2 particle, thus one can discuss the TPE contributions to the  $^3\text{He}$  in the same way as the one has been done for the nucleon. Here taking electron-nucleon scattering process  $e^-(p_1) + N(p_2) \rightarrow e^-(p_3) + N(p_4)$  for example, as one knows, after considering the TPE contributions, an extra term is introduced in the effective electromagnetic vertex of the nucleon and the vertex becomes:

$$\Gamma^\mu = \tilde{F}_1 \gamma^\mu + \tilde{F}_2 \frac{i\sigma^{\mu\nu} q_\nu}{2M} + \tilde{F}_3 \frac{\gamma \cdot K P^\mu}{M^2} \quad (1)$$

with  $M$  is the nucleon mass and the three independent momenta are  $q = p_1 - p_3$ ,  $K = p_1 + p_3$  and  $P = p_2 + p_4$ . The form factors  $\tilde{F}_i$ ,  $\{i = 1, 2, 3\}$  in above vertex are the functions of both the square of the momentum transfer  $Q^2$  and the photon polarization parameter  $\epsilon$ , which is related to the scattering angle by  $\epsilon = [1 + 2(1 + \tau) \tan^2(\theta/2)]^{-1}$ . The form factors  $\tilde{F}_{1,2}$  are usually recombined as  $\tilde{G}_{E,M}$  and  $\tilde{F}_3$  is expressed by  $Y_{2\gamma}$ . Moreover, the TPE contributions are separated from those based on one photon approximation, and one have,

$$\tilde{G}_{E,M}(Q^2, \epsilon) = G_{E,M}(Q^2) + \Delta G_{E,M}(Q^2, \epsilon), \quad Y_{2\gamma} = \frac{\nu}{M^2} \frac{\tilde{F}_3}{G_M}, \quad (2)$$

with  $\nu = P \cdot K$  and  $G_{E,M}$  are the electromagnetic form factors under one-photon approximation. With the contributions of the TPE process, the reduced differential cross section and the SSA can be expressed as:

$$\begin{aligned} \sigma_R &= G_M^2 + \frac{\epsilon}{\tau} G_E^2 + 2G_M \mathcal{R}(\Delta G_M + \epsilon G_M Y_{2\gamma}) + 2\frac{\epsilon}{\tau} G_E \mathcal{R}(\Delta G_E + G_M Y_{2\gamma}) + \mathcal{O}(e^4), \\ A_y &= \sqrt{\frac{2\epsilon(1+\epsilon)}{\tau}} \frac{1}{\sigma_R} \left\{ -G_M \mathcal{I}(\Delta G_E + G_M Y_{2\gamma}) + G_E \mathcal{I}(\Delta G_M + \left(\frac{2\epsilon}{1+\epsilon}\right) G_M Y_{2\gamma}) \right\}. \end{aligned} \quad (3)$$

In this work, we restrict ourself to low energy transfer region with  $Q^2 < 1 \text{ GeV}^2$ . Then in the calculations of the TPE corrections we only include the nucleon as the intermediate state. The Feynman diagrams are shown in Fig. 1. The TPE amplitudes corresponding to the diagrams are:

$$\mathcal{M}^{2\gamma} = Z^2 e^4 \int \frac{d^4 k}{(2\pi)^2} \left[ \frac{N_a(k)}{D_a(k)} + \frac{N_b(k)}{D_b(k)} \right]. \quad (4)$$

Here  $Z$  is the charge number of the targets, for the nucleon  $Z = 1$  and for the  $^3\text{He}$   $Z = 2$ . For the box diagram (as shown in Fig. 1 (a)), one has,

$$N_a = \bar{u}(p_3) \gamma_\mu (\hat{p}_1 - \hat{k}) \gamma_\nu u(p_1) \bar{u}(p_4) \Gamma_{1\gamma}^\mu(q - k) (\hat{p}_2 + \hat{k} + M) \Gamma_{1\gamma}^\nu(k) u(p_2),$$

$$D_a = [k^2 - \lambda^2][(k - q)^2 - \lambda^2][(p_1 - k)^2 - m^2][(p_2 + k)^2 - M^2]. \quad (5)$$

and in the same way one can get the expressions of  $N_b(k)$  and  $D_b(k)$  for the crossed box diagram (as shown in Fig. 1(b)). The electromagnetic vertex  $\Gamma_{1\gamma}^\mu(q)$  employed in Eq. (5) is the one under one-photon approximation. The form factors  $F_1$  and  $F_2$  are directly parameterized in terms of the sums of monopoles, of the form [10],

$$F_{1,2}(Q^2) = \sum_{i=1}^N \frac{n_i}{d_i + Q^2}, \quad (6)$$

where  $n_i$  and  $d_i$  are free parameters, and the normalization conditions are  $F_1^p = 1$  and  $F_2^p = \kappa_p$  for the proton,  $F_1^n = 0$  and  $F_2^n = \kappa_n$  for the neutron and  $F_1^{He} = 1$  and  $F_2^{He} = \kappa_{He}$  for the  $^3\text{He}$ , where  $\kappa_p = 1.793$ ,  $\kappa_n = -1.913$  and  $\kappa_{He} = -4.185$  are the proton, neutron and helium anomalous magnetic moments respectively. For the nucleon, we use the same parameters given by Ref. [10]. The parameters used in this work for the  $^3\text{He}$  [11] together with those for nucleon are list in Table 1.

Table 1: Parameters for the nucleon and the  $^3\text{He}$  form factors fitted in Eq. (6).  $n_i$  and  $d_i$  in units of  $\text{GeV}^2$ .

$N$	$F_1^p$	$F_2^p$	$F_1^n$	$F_2^n$	$F_1^{He}$	$F_2^{He}$
	3	3	3	2	3	3
$n_1$	0.38676	1.01650	24.8109	5.37640	3.58300	3.58307
$n_2$	0.53222	-19.0246	-99.8420	5.37640	0.19346	0.18396
$n_3$	-0.94491	18.0371	75.0544	--	-7.15263	-7.15242
$d_1$	3.29899	0.40886	1.98524	0.76533	0.25033	0.23274
$d_2$	0.45614	2.94311	1.72105	0.59289	3.60308	3.58744
$d_3$	3.32682	3.12550	1.64902	--	0.32599	0.29276

To carry out the TPE corrections to the SSAs for the nucleon and the  $^3\text{He}$ , the loop integrals are first evaluated analytically in terms of the four-point Passarino-Veltman functions [12] using the package FeynCalc [13]. Then, the Passarino-Veltman functions are evaluated numerically with LoopTools [14]. The numerical results about TPE corrections to the SSAs are displayed in the following sections.

### 3 Numerical Results and Discussions

In order to calculate the TPE corrections to the SSAs, we also have to consider the TPE corrections to the unpolarized differential cross sections. Similar to previous literatures [1, 5, 10], in the calculations of the unpolarized differential cross sections, the IR divergences in the TPE loop integral are canceled out by the standard MT corrections, which were introduced by L. M. Mo and Y. S. Tsai [15, 16] and had been included in the experiment. As one knows, the soft part of the TPE corrections, which contains all the information on IR divergences of the loop integral, can be expressed as  $\mathcal{M}_{2\gamma}^{soft} = \delta^{soft} M^{1\gamma}$ . That means the soft part of the TPE corrections contributes to  $F_1$  and  $F_2$  with same factor  $\delta^{soft}$ . Then correspondingly, one can conclude that the soft part of the TPE corrections to the electromagnetic form factors are,

$$\Delta G_E^{soft}/G_E \equiv \Delta G_M^{soft}/G_M = \delta^{soft}. \quad (7)$$

As shown in Eq. (3), the SSA is related to the imaginary part of the TPE corrections, and the IR divergent part of the TPE corrections only contributes to the electromagnetic form factors. Then we can

rewrite it as,

$$A_y = \sqrt{\frac{2\epsilon(1+\epsilon)}{\tau}} \frac{1}{\sigma_R} \left\{ G_E G_M [\mathcal{I}(\Delta G_M)/G_M - \mathcal{I}(\Delta G_E)/G_E] + G_M \left[ \frac{2\epsilon}{1+\epsilon} G_E - G_M \right] \mathcal{I}(Y_{2\gamma}) \right\}. \quad (8)$$

The second squared bracket only relates to  $Y_{2\gamma}$  (or  $\tilde{F}_3$ ), which is IR finite. Taking Eq. (7) into the first squared bracket one can see the soft part of TPE corrections has no contributions to the SSA, that means the TPE corrections to the terms in the brace are IR finite and no more considerations about IR divergence are needed.

As we mentioned in previous section, the expression used to evaluate the TPE corrections to the  ${}^3\text{He}$  are the same as those for the nucleon. In actual calculations, we only replace the nucleon mass, nucleon charge number and form factors by the corresponding quantities of the  ${}^3\text{He}$  in Eqs. (1) - (5). Detailedly, the mass of the  ${}^3\text{He}$  is about 3 times larger than the nucleon mass and the charge of the  ${}^3\text{He}$  is  $2e$ . Moreover the electromagnetic form factors of the  ${}^3\text{He}$  are somewhat softer than the nucleon form factors and have zeros at  $Q^2 \simeq 0.45 \text{ GeV}^2$  and  $Q^2 \simeq 0.7 \text{ GeV}^2$  for the charge and magnetic form factors respectively [17].

The  $\theta$  dependence of the TPE contributions to the SSAs for the nucleon and the  ${}^3\text{He}$  are displayed in Figs. 2 - 4. For  $Q^2 = 0.2 \text{ GeV}^2$ , as shown in Fig. 2, the TPE contributions to the SSAs for both the proton and the neutron are positive and increase with the increasing of the scattering angle  $\theta$ , and reach about 1% for the proton and 0.25% for the neutron in the backward limit. While the SSA for the  ${}^3\text{He}$  is negative and decreases with the increasing of  $\theta$  and at about  $\theta = 135^\circ$ , it reaches minimum value of approximately 1.6%. For  $Q^2 = 0.5 \text{ GeV}^2$  (Fig. 3) and  $Q^2 = 1.0 \text{ GeV}^2$  (Fig. 4), the TPE contributions to the SSAs for the proton are positive while for the neutron are negative and moreover, the absolute values decrease with the increasing of the scattering angle. At the forward limit, the absolute values of the TPE corrections to the SSAs for the proton (neutron) are less than 0.2% (0.15%) at  $Q^2 = 0.5 \text{ GeV}^2$  and more than 0.4% (about 0.4%) at  $Q^2 = 1.0 \text{ GeV}^2$ . For the  ${}^3\text{He}$ , the tendency of the curves are similar to the one at  $Q^2 = 0.2 \text{ GeV}^2$  and the minimum values are 15% and 3% at  $Q^2 = 0.5 \text{ GeV}^2$  and  $Q^2 = 1.0 \text{ GeV}^2$  respectively. From these figures, one can conclude the TPE contributions to SSAs for the  ${}^3\text{He}$  are strongly dependent on the scattering angle and their amplitudes are much larger than those for the nucleon. One reason is that the charge of the  ${}^3\text{He}$  is  $2e$  this produces a factor 4 in the TPE amplitudes. Another is that the form factors of the  ${}^3\text{He}$  are much softer than those of the nucleon, thus the contributions from the TPE process with the two photon sharing the momentum transfer are large.

In the deep inelastic scattering language, the nucleon structures are described by four independent functions  $W_1$ ,  $W_2$ ,  $G_1$  and  $G_2$ . The first two are unpolarized structure functions while the rest two are the polarized ones. Generally, the polarized structure functions are represented by the dimensionless functions  $g_1 = M^2 \nu G_1$  and  $g_2 = M \nu^2 G_2$ . In the deep inelastic region, the structure functions  $g_{1,2}$  are only depend on the Bjorken variable  $x = Q^2/2M\nu$ . However, this scaling behavior breaks down in non-perturbative QCD, thus  $g_{1,2}$  are functions of both  $x$  and  $Q^2$ . In the naive quark model, where the quarks are completely independent and gluons are not considered,  $g_2$  is expected to be zero. In this case, the SSA,  $A_y$ , is directly proportional to the structure function  $g_1$ .

In general, the spin structure functions of the  ${}^3\text{He}$ ,  $g_1^{{}^3\text{He}}$ , can be represented as the convolution of those of the neutron  $g_1^n$  and of the proton  $g_1^p$  with the spin-dependent nucleon light-cone momentum distributions  $\Delta f_{N/{}^3\text{He}}(y)$ , where  $y$  is the ratio of the struck nucleon to the nucleus light-cone plus components of the momenta [18–21],

$$g_1^{{}^3\text{He}}(x, Q^2) = \int_x^3 \frac{dy}{y} \left[ \Delta f_{n/{}^3\text{He}}(y) g_1^n(x/y, Q^2) + \Delta f_{p/{}^3\text{He}}(y) g_1^p(x/y, Q^2) \right]. \quad (9)$$

Detailed calculations [18–20] by various groups using different ground-state wave functions of the  ${}^3\text{He}$  came to a similar conclusion that  $\Delta f_{N/{}^3\text{He}}$  are sharply peaked around  $y \simeq 1$  due to the small average

separation energy per nucleon. Thus Eq. (9) can be approximated by [21],

$$g_1^{3\text{He}}(x, Q^2) = P_n g_1^n(x, Q^2) + 2P_p g_1^p(x, Q^2), \quad (10)$$

with  $P_n$  ( $P_p$ ) are the effective polarizations of the neutron (proton) inside the polarized  $^3\text{He}$ . Considering the ground state wave function of the  $^3\text{He}$ , which corresponds to  $S$ -wave type interaction between any pair of the nucleons inside the  $^3\text{He}$ , only the neutron is polarized. Thus, one has  $P_n = 1$  and  $P_p = 0$ . In practice, the wave function of the  $^3\text{He}$  include also higher partial waves, namely the  $D$  and  $S'$  partial waves, this leads to the depolarization of spin of the neutron and polarization of the protons in the  $^3\text{He}$ . The average of calculations with several models can be summarized as  $P_n = 0.86 \pm 0.02$  and  $P_p = -0.028 \pm 0.004$  [22].

According to Eq. (10) and the approximation that the SSA  $A_y$  is proportional to the polarized structure  $g_1$ , one has,

$$A_y^{3\text{He}} = \frac{\sigma^n}{\sigma^{3\text{He}}} P_n A_y^n + 2 \frac{\sigma^p}{\sigma^{3\text{He}}} P_p A_y^p, \quad (11)$$

where  $\sigma^n$ ,  $\sigma^p$  and  $\sigma^{3\text{He}}$  are the unpolarized differential cross sections for the neutron, proton and  $^3\text{He}$ . In present work, we first estimate the TPE corrections to the SSAs for the  $^3\text{He}$  directly from Eq. (4) and also we can calculate  $A_y^{3\text{He}}$  from Eq. (11) based on the TPE corrections to the SSAs for the nucleon.

The  $Q^2$  dependences of the TPE corrections to the SSAs for the  $^3\text{He}$  at different scattering angles are displayed in Figs. 5 - 7. In these figures,  $A_y^{(a)}$  means the TPE corrections to the SSAs for the  $^3\text{He}$  obtained directly from Eq. (4), which are corresponding to the solid curves in the figures. While  $A_y^{(b)}$  refers to the SSAs for the  $^3\text{He}$  estimated from Eq. (11) based on the TPE corrections to the SSAs for the nucleon. From these figures one can see, in the region with  $Q^2$  under  $0.1 \text{ GeV}^2$ , the SSAs for the  $^3\text{He}$  are very close to zero and in this region the results obtained from two different methods are consistent with each other. For the solid curves, one can see, they all have deep dips in the range  $0.4 \text{ GeV}^2 < Q^2 < 0.5 \text{ GeV}^2$ . For  $\theta = \pi/10$ , the dip appears at  $Q^2 \simeq 0.4 \text{ GeV}^2$  and the minimum value is about 3%. While for  $\theta = \pi/3$ , at  $Q^2 \simeq 0.43 \text{ GeV}^2$ , the SSA  $A_y^{(a)}$  reaches minimum value of approximately  $-8\%$  and for  $\theta = 2\pi/3$ ,  $A_y^{(a)}$  reaches its minimum at  $Q^2 \simeq 0.5 \text{ GeV}^2$  with the value about  $-11\%$ . These dips can be well explained by the zero point of the charge form factor of the  $^3\text{He}$  at  $Q^2 \simeq 0.45 \text{ GeV}^2$ . With  $Q^2$  increasing, the solid curves go up quickly, and in the region around  $0.8 \text{ GeV}^2$ , they begin to drop again, this can be interpreted as the reflection of zero point of the  $^3\text{He}$  magnetic form factor at  $Q^2 \simeq 0.7 \text{ GeV}^2$ .

In Figs. 5 - 7, the dashed curves, which correspond with the SSAs for the  $^3\text{He}$  obtained from Eq. (11), drop quickly in the range  $Q^2 > 0.2 \text{ GeV}^2$ . This feature is the same with the one of the solid curves. However, as one can see from these figures, the  $A_y^{(b)}$  monotonically decreases with  $Q^2$  increasing and quantitatively reaches several hundred percent at  $Q^2 = 1 \text{ GeV}^2$ , which is not consistent with the solid curves. In Eq. (11), the effective polarizations of the proton is only  $1/30$  of the neutron, that means, the polarization of neutron is more important inside the polarized  $^3\text{He}$ . Thus, one has  $A_y^{3\text{He}} \sim \sigma^n / \sigma_{3\text{He}} P_n A_y^n$ . In Fig. 8, we shown the differential cross section ratio of the neutron to the  $^3\text{He}$  at different scattering angles. We see that the form factors of the  $^3\text{He}$  is much softer than the nucleon (except the neutron electric form factor), that leads the ratio  $\sigma^n / \sigma_{3\text{He}}$  increases rapidly with the  $Q^2$  increasing. From the figure, one can find, in the range  $Q^2 > 0.4 \text{ GeV}^2$  the differential cross section of neutron is at least two orders larger than those of the  $^3\text{He}$  for  $\theta = \pi/10$  and  $\pi/3$ . Even for  $\theta = 2\pi/3$ , the differential cross section ratio of neutron to  $^3\text{He}$  is also at least 30. Such a large ratio leads to the SSAs for  $^3\text{He}$  obtained from Eq. (11) decreases rapidly with the increasing of  $Q^2$ . Above all, in Eq. (11), the SSA for the  $^3\text{He}$  is just approximately equal the the sum of the contributions from the proton and neutron. Eq. 11 had only been verified in the  $Q^2$  range from several  $\text{GeV}^2$  to about  $10 \text{ GeV}^2$  [21]. The validity of this approximation keeps unknown in the low energy transfer region. In Figs. 5-7, we believe the results from two different methods are consistent under  $0.1 \text{ GeV}^2$  just because the TPE contributions are nearly invisible in such low energy transfer region. Moreover, in the right-hand side of Eq. (11), for the calculations of the SSAs for the nucleon contributed from the TPE process, only the elastic contribution has been considered.

The corrections from the nucleon resonances, such as  $\Delta(1232)$  are expected to revise the results within a specific limits. Thus, in the present work, we prefer the results from the direct calculation of Eq. (4). Furthermore, the calculations within the plain wave impulse approximation [19,23,24], in which the nuclear current arise from the one-nucleon current and the residual nucleus is assumed not participate in the scattering process, may provide more accurate information on TPE corrections to SSA for  $^3\text{He}$ .

To summarize, we have studied the TPE corrections to the SSAs for the nucleon and the  $^3\text{He}$  in a simple hadronic model, and in present calculations only the elastic contributions are considered. The SSAs for the nucleon are found to be rather small, while for the  $^3\text{He}$  are rather large. Another important feature of the SSA for  $^3\text{He}$  is its strong dependence of the momentum transfer. From our calculations, one can conclude that the SSAs for the  $^3\text{He}$  should be more easily measured in the scattering angle range  $120^\circ < \theta < 150^\circ$  and momentum transfer range from  $0.3 \text{ GeV}^2$  to  $0.6 \text{ GeV}^2$  in the experiments. We also try to estimate the SSA for the  $^3\text{He}$  from the contributions of its nucleon component based on a very simple approximate equation. The results obtained from this approximation are comparable to those from the direct calculations of the TPE process at very small  $Q^2$  region. However, large discrepancies between the results from the two methods are presented at the range  $Q^2 > 0.3 \text{ GeV}^2$ . Further study of the SSAs for the  $^3\text{He}$  based on the plane wave impulse approximation are needed.

## 4 Acknowledgments

We thank P. G. Blunden and J. P. Chen for helpful discussions and W. Melnitchouk for his  $^3\text{He}$  form factors parameterizations. This work is partly supported by the National Sciences Foundations of China under grants No. 10775148,10975146. The authors are also grateful to the CAS for grant No KJCX3-SYW-N2.

## References

- [1] P. G. Blunden, W. Melnitchouk and J. A. Tjon, Phys. Rev. Lett. **91**, 142304 (2003).
- [2] P. A. M. Guichon and M. Vanderhaeghen, Phys. Rev. Lett. **91**, 142303 (2003).
- [3] Y. -C. Chen, A. Afanasev, S. J. Brodsky, C. E. Carlson and M. Vanderhaeghen, Phys. Rev. Lett. **93**, 122301 (2004).
- [4] S. Kondratyuk, P. G. Blunden, W. Melnitchouk and J. A. Tjon, Phys. Rev. Lett. **95**, 172503 (2005).
- [5] S. Kondratyuk and P. G. Blunden, Phys. Rev. C **75**, 038201 (2007).
- [6] A. V. Afanasev, S. J. Brodsky, *et al.*, Phys. Rev. D **72**, 013008 (2005).
- [7] <http://hallaweb.jlab.org/experiment/E05-102/e05-015/index.html>
- [8] S. Platchkov *et al.*, Nucl. Phys. A **510**, 740 (1990).
- [9] B. Blankleider and R. M. Woloshyn, Phys. Rev. C **29** 538 (1984).
- [10] P. G. Blunden, W. Melnitchouk and J. A. Tjon, Phys. Rev. C **72**, 034612 (2005).
- [11] W. Melnitchouk and P. G. Blunden, private communication.
- [12] G. Passarino and M. Veltman, Nucl. Phys. B **160**, 151 (1979).
- [13] R. Mertig, M. Bohm and A. Denner, Comput. Phys. Commun. **64**, 345 (1991).
- [14] T. Hahn, M. Perez-Victoria, Comput. Phys. Commun. **118**, 153 (1999).

- [15] Y. S. Tsai, Phys. Rev. 122 (1961) 1898.
- [16] L. W. Mo and Y. S. Tsai, Rev. Mod. Phys. 41 (1969) 205.
- [17] A. Amroun et al., Nucl. Phys. A **579**, 596 (1994).
- [18] C. Ciofi degli Atti, S. Scopetta, E. Pace, and G. Salme, Phys. Rev. C **48**, 968 (1993).
- [19] R. W. Schülzke and P. U. Sauer, Phys. Rev. C **48**, 38 (1993).
- [20] F. Bissey, A. W. Thomas, and I. R. Afnan, Phys. Rev. C **64**, 024004 (2001).
- [21] F. Bissey, V. Guzey, M. Strikman, and A. Thomas, Phys. Rev. C **65**, 064317 (2002).
- [22] J. L. Friar, B. F. Gibson, G. L. Payne, A. M. Bernstein, and T. E. Chupp, Phys. Rev. C **42** 2310 (1990).
- [23] A. Kievsky, E. Pace, G. Salme, and M. Viviani, Phys. Rev. C **56**, 64 (1997).
- [24] C. Ciofi degli Atti, E. Pace, and G. Salme, Phys. Rev. C **46**, R1591 (1992); **51**, 1108 (1995)

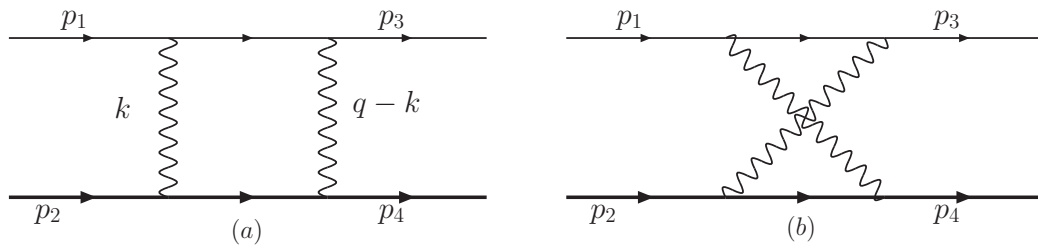


Fig. 1: Feynman diagram used in present calculations.

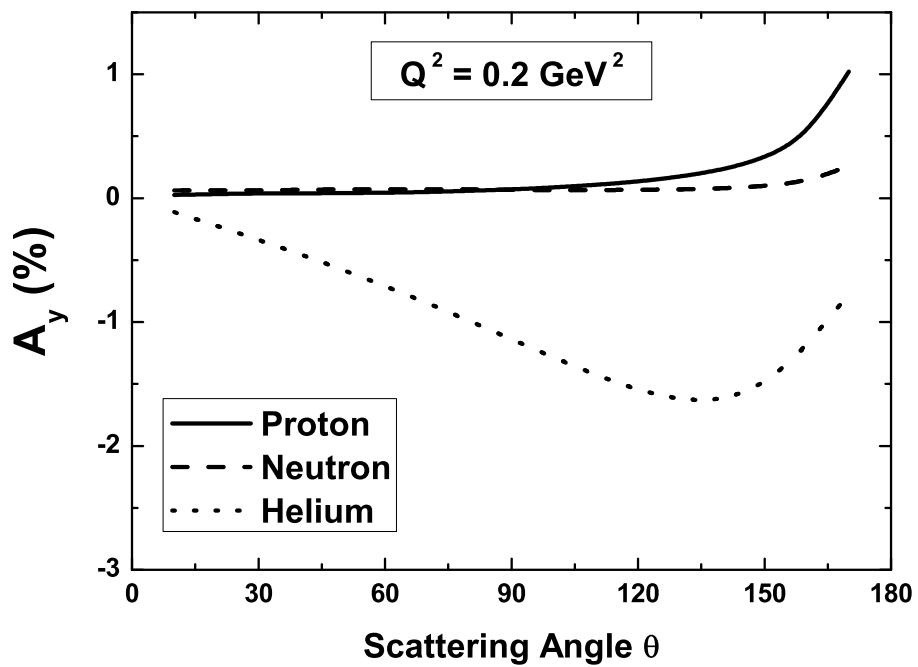


Fig. 2: The TPE contributions to the SSAs for the nucleon and the  ${}^3\text{He}$  at  $Q^2 = 0.2 \text{ GeV}^2$ .

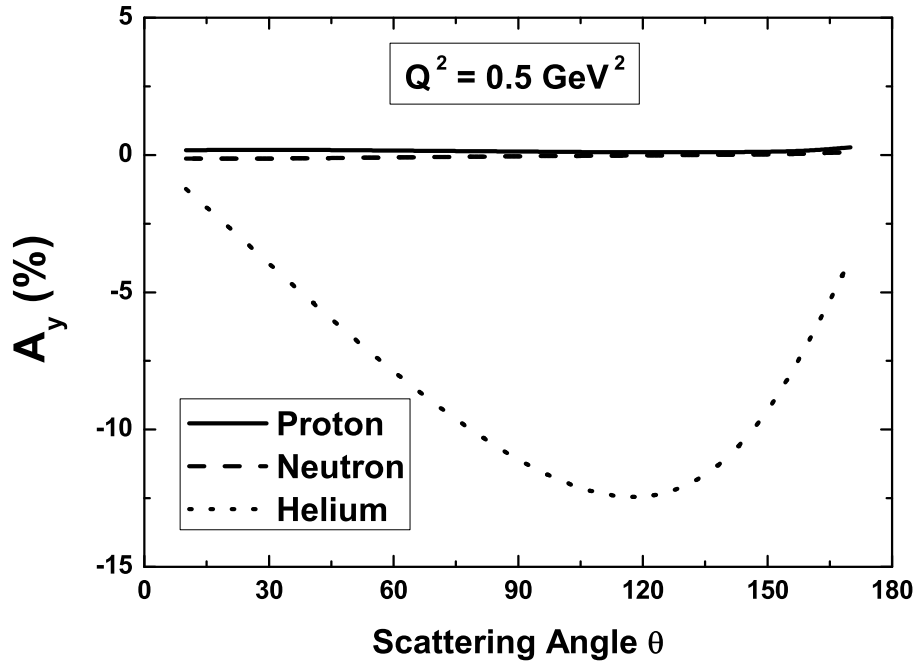


Fig. 3: The same as Fig. 2 but for  $Q^2 = 0.5 \text{ GeV}^2$ .

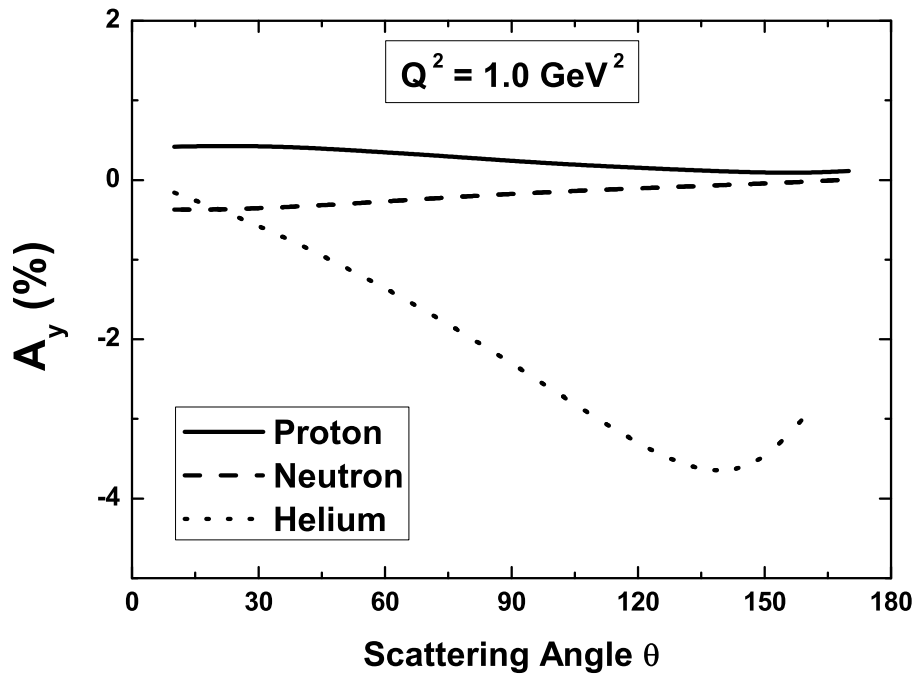


Fig. 4: The same as Fig. 2 but for  $Q^2 = 1.0 \text{ GeV}^2$ .

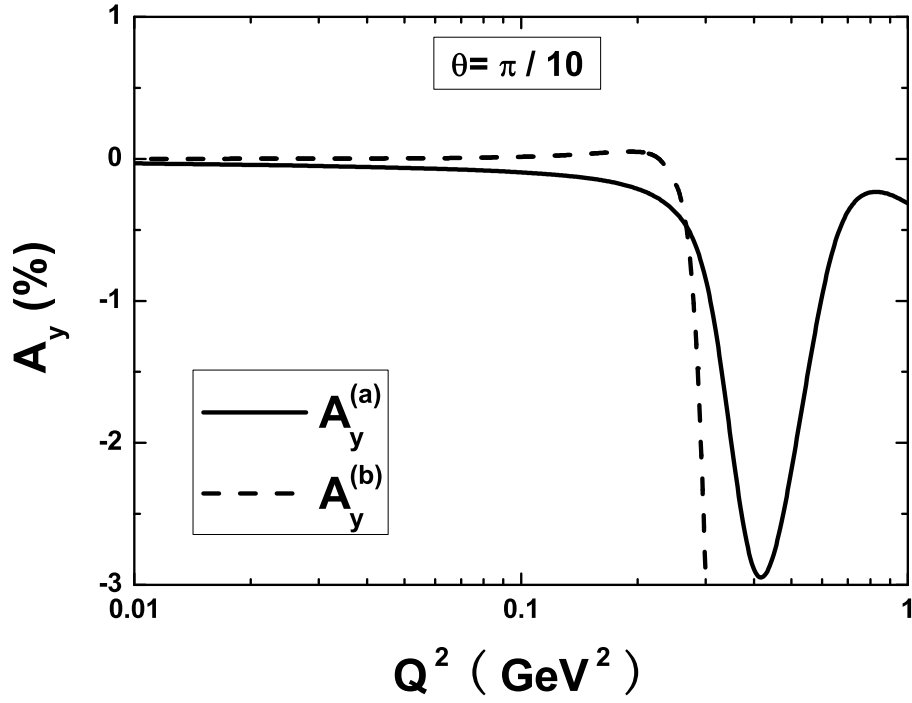


Fig. 5: The  $Q^2$  dependence of the TPE contributions to the SSA for the  ${}^3\text{He}$  at  $\theta = \pi/10$ .  $A_y^{(a)}$  is the result from a direct estimation of the TPE contributions, while  $A_y^{(b)}$  is the result obtained from Eq. (11).

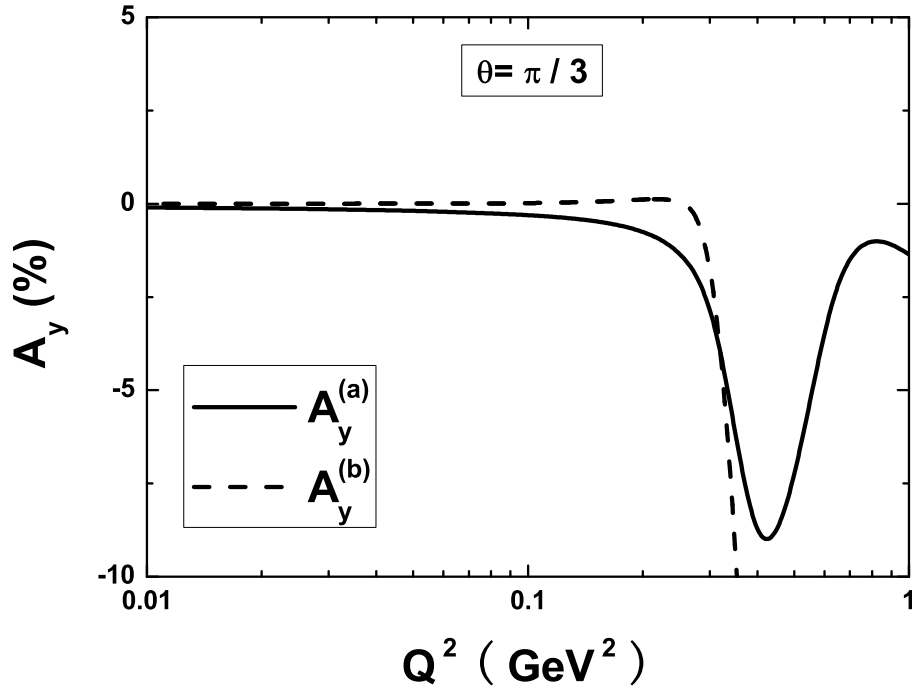


Fig. 6: The same as Fig. 5 but for  $\theta = \pi/3$ .

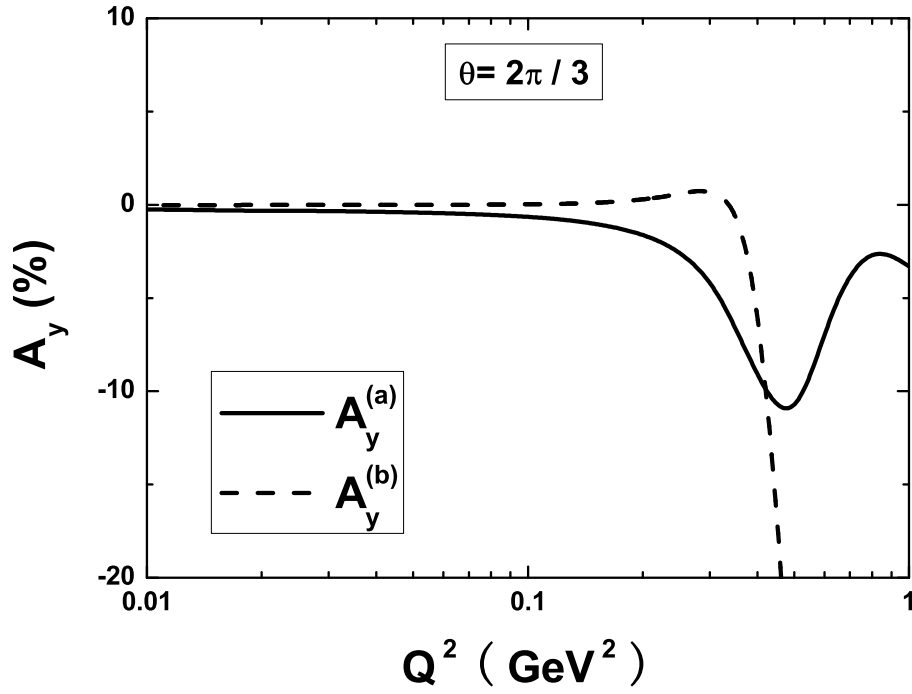


Fig. 7: The same as Fig. 5 but for  $\theta = 2\pi/3$ .

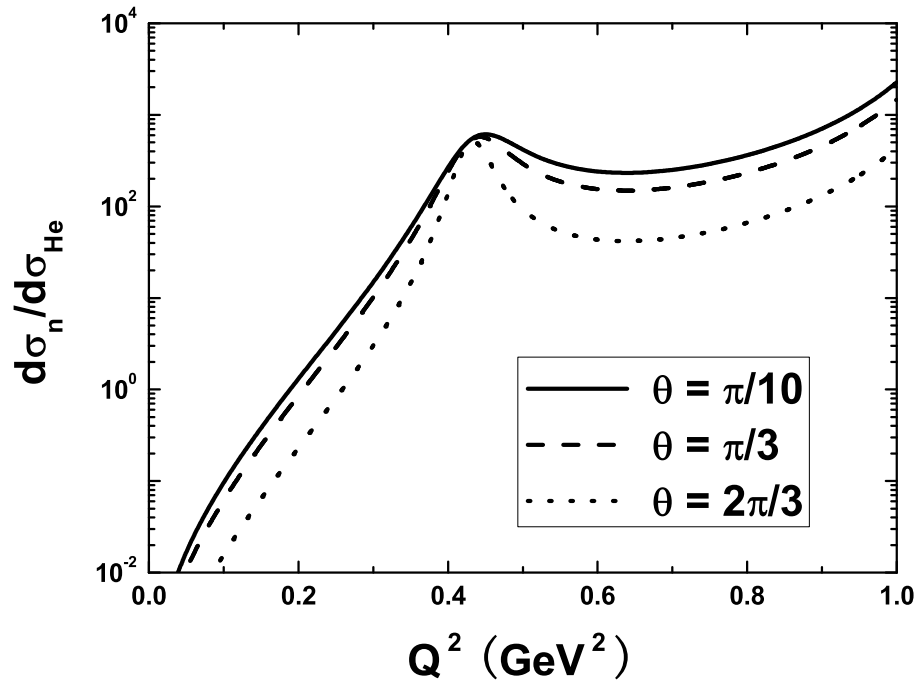


Fig. 8: The differential cross section ratio of the neutron and the  ${}^3\text{He}$  at the different scattering angle.